Ontogenetic development of highly variable ceratitid ammonoids from the Anisian (Middle Triassic) of Nevada, USA (#54008)

First submission

Guidance from your Editor

Please submit by 11 Dec 2020 for the benefit of the authors (and your \$200 publishing discount).



Structure and Criteria

Please read the 'Structure and Criteria' page for general guidance.



Custom checks

Make sure you include the custom checks shown below, in your review.



Raw data check

Review the raw data.



Image check

Check that figures and images have not been inappropriately manipulated.

Privacy reminder: If uploading an annotated PDF, remove identifiable information to remain anonymous.

Files

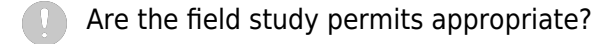
Download and review all files from the <u>materials page</u>.

- 11 Figure file(s)
- 3 Table file(s)
- 1 Raw data file(s)



Field study

Have you checked the authors field study permits?



Structure and Criteria



Structure your review

The review form is divided into 5 sections. Please consider these when composing your review:

- 1. BASIC REPORTING
- 2. EXPERIMENTAL DESIGN
- 3. VALIDITY OF THE FINDINGS
- 4. General comments
- 5. Confidential notes to the editor
- Prou can also annotate this PDF and upload it as part of your review

When ready <u>submit online</u>.

Editorial Criteria

Use these criteria points to structure your review. The full detailed editorial criteria is on your guidance page.

BASIC REPORTING

- Clear, unambiguous, professional English language used throughout.
- Intro & background to show context.
 Literature well referenced & relevant.
- Structure conforms to <u>PeerJ standards</u>, discipline norm, or improved for clarity.
- Figures are relevant, high quality, well labelled & described.
- Raw data supplied (see <u>PeerJ policy</u>).

EXPERIMENTAL DESIGN

- Original primary research within Scope of the journal.
- Research question well defined, relevant & meaningful. It is stated how the research fills an identified knowledge gap.
- Rigorous investigation performed to a high technical & ethical standard.
- Methods described with sufficient detail & information to replicate.

VALIDITY OF THE FINDINGS

- Impact and novelty not assessed.
 Negative/inconclusive results accepted.
 Meaningful replication encouraged where rationale & benefit to literature is clearly stated.
- All underlying data have been provided; they are robust, statistically sound, & controlled.
- Speculation is welcome, but should be identified as such.
- Conclusions are well stated, linked to original research question & limited to supporting results.

Standout reviewing tips



The best reviewers use these techniques

Τ	p

Support criticisms with evidence from the text or from other sources

Give specific suggestions on how to improve the manuscript

Comment on language and grammar issues

Organize by importance of the issues, and number your points

Please provide constructive criticism, and avoid personal opinions

Comment on strengths (as well as weaknesses) of the manuscript

Example

Smith et al (J of Methodology, 2005, V3, pp 123) have shown that the analysis you use in Lines 241-250 is not the most appropriate for this situation. Please explain why you used this method.

Your introduction needs more detail. I suggest that you improve the description at lines 57-86 to provide more justification for your study (specifically, you should expand upon the knowledge gap being filled).

The English language should be improved to ensure that an international audience can clearly understand your text. Some examples where the language could be improved include lines 23, 77, 121, 128 - the current phrasing makes comprehension difficult.

- 1. Your most important issue
- 2. The next most important item
- 3. ...
- 4. The least important points

I thank you for providing the raw data, however your supplemental files need more descriptive metadata identifiers to be useful to future readers. Although your results are compelling, the data analysis should be improved in the following ways: AA, BB, CC

I commend the authors for their extensive data set, compiled over many years of detailed fieldwork. In addition, the manuscript is clearly written in professional, unambiguous language. If there is a weakness, it is in the statistical analysis (as I have noted above) which should be improved upon before Acceptance.



Ontogenetic development of highly variable ceratitid ammonoids from the Anisian (Middle Triassic) of Nevada, USA

Eva Alexandra Bischof Corresp., 1, Nils Schlüter 2, Dieter Korn 2, Jens Lehmann 1

Corresponding Author: Eva Alexandra Bischof Email address: bischof@uni-bremen.de

Ammonoids reached their greatest diversity during the Triassic period. In the early Middle Triassic (Anisian) stage ammonoid diversity was mainly dominated by representatives of the family Ceratitidae. This high taxonomic diversity is, however, decoupled from their morphologic disparity. Therefore, the high diversity of ceratitids of the Anisian of Nevada, was initially assumed to be reasoned in artificial over-splitting of this group due to its high phenotypic variability. This study aims to contribute to this issue by applying geometric morphometrics methods, using landmarks and semi-landmarks, in the study of ontogenetic cross-sections of ammonoids for the first time. The results reveal that alterations in ontogenetic trajectories, linked to heterochronic processes, lead to the phenotypic diversification of the species studied herein. Our knowledge, based on these ontogenetic changes, challenge the traditional treatment of species using solely adult characters for their distinction. This study highlights the importance of analyzing inter- and intraspecific variation of ceratitid assemblages considering their ontogenetic development. Furthermore, this study demonstrates that the high diversity of the Anisian ammonoid assemblages of Nevada based on the traditional nomenclatoric approach is regarded to be reasonably accurate.

 $^{^{}m 1}$ Geowissenschaftliche Sammlung, FB5 Geowissenschaften, Universität Bremen, Bremen, Bremen, Germany

² Museum für Naturkunde, Leibniz-Institut für Evolutions- und Biodiversitätsforschung, Humboldt Universität Berlin, Leibniz-Institut für Evolutions- undBiodiversitätsforschung, Invalidenstraße, 43, 10115 Berlin, Germany, Berlin, Germany



1 Ontogenetic development of highly variable ceratitid

2 ammonoids from the Anisian (Middle Triassic) of

Nevada, USA

4 5 6

3

Eva A. Bischof¹, Nils Schlüter², Dieter Korn², Jens Lehmann¹

7

- 8 ¹ Geowissenschaftliche Sammlung, Fachbereich Geowissenschaften, Universität Bremen,
- 9 Leobener Strasse 8, 28357 Bremen, Germany
- 10 ² Naturhistorisches Forschungsinstitut, Museum für Naturkunde, Humboldt-Universität
- 11 zu Berlin, Invalidenstraße 43, 10115 Berlin, Germany

12

- 13 Corresponding Author:
- 14 Eva Bischof¹
- 15 MARUM, Leobener Strasse 8, 28359 Bremen, Germany
- 16 Email address: eva.bischof@hotmail.com

17 18

Abstract

- 19 Ammonoids reached their greatest diversity during the Triassic period. In the early Middle
- 20 Triassic (Anisian) stage ammonoid diversity was mainly dominated by representatives of the
- 21 family Ceratitidae. This high taxonomic diversity is, however, decoupled from their morphologic
- 22 disparity. Therefore, the high diversity of ceratitids of the Anisian of Nevada was initially
- 23 assumed to be reasoned in artificial over-splitting of this group due to its high phenotypic
- variability. This study aims to contribute to this issue by applying geometric morphometrics
- 25 methods, using landmarks and semi-landmarks, in the study of ontogenetic cross-sections of
- ammonoids for the first time. The results reveal that alterations in ontogenetic trajectories, linked
- 27 to heterochronic processes, lead to the phenotypic diversification of the species studied herein.
- 28 Our knowledge, based on these ontogenetic changes, challenge the traditional treatment of
- 29 species using solely adult characters for their distinction. This study highlights the importance of
- 30 analyzing inter- and intraspecific variation of ceratitid assemblages considering their ontogenetic
- 31 development. Furthermore, this study demonstrates that the high diversity of the Anisian
- 32 ammonoid assemblages of Nevada based on the traditional nomenclatoric approach is regarded
- 33 to be reasonably accurate.

34 35

Introduction

- 36 After the Permian-Triassic mass extinction event, ammonoids flourished and spread globally to
- become an important part of the marine biota (Brayard & Bucher 2015; Brosse et al. 2013;
- House 1993; Neige 2015). They reached their greatest generic diversity of all times in the
- 39 Triassic Period (Brayard et al. 2009; Whiteside & Ward 2011). The diversity peak in the late



- Anisian is mainly dominated by genera of one family: The Ceratitidae (Bravard et al. 2009: 40
- supporting material fig. S2). Not least due to their wide paleogeographic distribution, and high 41
- diversity and abundance in the fossil record, ammonoids are an excellent biostratigraphic tool. 42
- Especially, the discoidal-shaped members of the family Ceratitidae (Mojsisovics 1879) are 43
- 44 namesake for many North-American Anisian biostratigraphic zones and subzones (Jenks et al.
- 2015); figs. 13.13, 13.14). 45
- 46 The fossil material used in this study was collected in the late Anisian Fossil Hill Member of the
- Star Peak Basin in north-western Nevada, USA. The studied successions are considered to be the 47
- world's most complete low-paleolatitude successions, revealing late Anisian ammonoid 48
- 49 assemblages (Monnet & Bucher 2005). The first comprehensive taxonomic work on the Anisian
- ammonoid communities of the famous fossil locality at Fossil Hill in the Humboldt Range was 50
- published by Smith (1914) in his monograph on the North American Middle Triassic marine 51
- 52 invertebrates. According to the taxonomic practice of his time, he described or listed a total of
- 53 110 ammonoid species from Fossil Hill. More recently, Silberling & Nichols (1982), Bucher
- 54 (1992) and Monnet & Bucher (2005) refined the original alpha taxonomy and the biostratigraphy
- with contemporaneous methods and reduced the number to 81 valid species (Brosse et al. 2013). 55
- However, it is important to note that succeding assemblages show a progressive shift in 56
- morphology; therefore, the cutoff between contiguous species is essentially arbitrary (Silberling 57
- 1962; Silberling & Nichols 1982). This challenges the taxonomic concept and sheds new light on 58
- diversity patterns in general. An increasing number of studies suggest that the high diversity 59
- could in some cases be artificially inflated by taxonomic over-splitting (De Baets et al. 2013; 60
- 61 Forey et al. 2004; Knauss & Yacobucci 2014). Furthermore, taxonomic diversity and
- 62 morphological disparity of Triassic ammonoids were probably decoupled (Brosse et al. 2013;
- McGowan 2004; McGowan 2005). At present, only few studies have investigated trends in 63
- morphological disparity of Triassic ammonoids (Monnet et al. 2015). 64
- Previous studies have proven that particularly due to their accretionary planispiral conch 65
- 66 growth with conservation of previous growth stages - ammonoids offer a high-resolution data
- basis for ontogenetic, developmental and also taxonomic studies. While the study of conch 67
- ontogeny has a long history in the study of Paleozoic ammonoids (reviews by Korn 2010; Korn 68
- & Klug 2007), it was only rarely done with Mesozoic ammonoids (e.g., Bischof & Lehmann 69
- 70 2020; Monnet et al. 2011; Naglik et al. 2015; Rieber 1962; Tajika et al. 2015). So far, the
- morphology and ontogeny of ammonoids was mainly assessed using descriptive, comparative or 71
- traditional morphometric methods (linear measurements). Klug et al. (2015); (Korn 2010); Korn 72
- & Klug (2003); and Korn & Klug (2007) developed the so-called Raupian parameters (Raup 73
- 74 1966) that were initially introduced to describe the coiled conch morphospace. However, the
- shapes of discoidal ammonoids often differ through their characteristic ways of ventral arching 75
- 76 and presence or absence of a keel. Both characteristics can hardly be described with linear
- measurements (Neige 1999). Therefore, the use of traditional morphometric methods is limited 77
- 78 when it comes to distinguishing ceratitid species.



- 79 In this study, for the first time the morphology and ontogeny of whorl profiles of the late Anisian
- 80 family Ceratitidae was analyzed using a landmark-based geometric morphometric methods
- 81 (GMM), instead of linear measurements (traditional morphometrics). This is reasoned in the
- 82 tremendous advantages of GMM over the latter; landmarks and semi-landmarks cover shape
- variations of complete morphologies, which are sometimes not to be recognized or overseen with
- linear measurements of traditional morphometrics methods (Neige 1999). However, GMM can
- 85 not only be adapted more flexibly to individual requirements, but are also easier to use for
- statistical analysis and allow to analyze shape and size separately (Hammer & Harper 2005). In
- 87 addition, landmark-based methods do not introduce artifactual patterns of covariation (Gerber
- 88 2017) which is often the case when proportions are studied.
- 89 The literature of landmark-based approaches in morphological analyses of molluscs is rather
- 90 scarce. Although important pioneering works exist, the previous studies are of limited use in an
- 91 ontogenetic context because they all focus either on the shape of the whole conch or on single
- 92 (isolated) ontogenetic stages (e.g., Johnston et al. 1991; Knauss & Yacobucci 2014; Neige 1999;
- 93 Neige & Dommergues 1995; Reyment 2003; Reyment & Kennedy 1998; Stone 1998; Van
- 94 Bocxlaer & Schultheiß 2010).
- 95 The present study is one of the first to analyze ontogenetic series of ammonoid conch cross
- 96 sections using geometric morphometrics methods. While previous studies used the method of
- 97 Fourier Analysis for the outline analysis of ammonoid whorl profiles of adult conchs (Courville
- 98 & Crônier 2005; Korn & Klug 2012; Simon et al. 2010; Simon et al. 2011) and also of
- ontogenetic stages (Klein & Korn 2014), this study uses a combined landmark and semi-

100 landmark approach.

- 101 In order to evaluate the hitherto used taxonomic scheme, ontogenetic patterns within the family
- 102 Ceratitidae and their changes over time were investigated. Working with ontogenetic cross-
- sections allows to estimate the relative age of the whorls, which adds an extra dimension to the
- analysis. The tools presented here are intended to complement traditional descriptions and to
- objectify and quantify their results. This study should serve as a general motivation to conduct
- 106 GMM studies on invertebrates with accretionary planispiral growth.

107108

Materials & Methods

- 109 **Geological setting.** The ammonoid material derives from the Fossil Hill Member of Fossil Hill
- in the Humboldt Range and Muller Canyon in the Augusta Mountains (Pershing County), north-
- western Nevada, USA (Fig. 1) and is stored in the Geosciences Collection of the University of
- 112 Bremen (GSUB), Germany. The material from the Wilderness Study Area of the Augusta
- 113 Mountains, Pershing County was collected with permission of the U.S. Department of the
- 114 Interior, Bureau of Land Management (BLM, Nevada State office, Winnemucca District). The
- Fossil Hill Member is a succession of alternating layers of mudstone with lenticular limestone
- and calcareous siltstone beds (see Fig. 2). The rich and diverse fossil content consists primarily
- of halobiid bivalves and ammonoids. Detailed geological and stratigraphic descriptions were



- published by Nichols & Silberling (1977), Silberling & Nichols (1982) and Monnet & Bucher
- 119 (2005).
- 120 Studied specimens. The fossil material comprises 72 ammonoid specimens of the family of
- 121 Ceratitidae Mojsisovics 1879. These are representing 12 species in 7 genera (Fig. 2, Tab. 1) that
- either belong to the subfamily Beyrichitinae Spath 1934 or Paraceratitinae Silberling 1962. Most
- of the studied species show high intraspecific variation with overlapping morphologies (see Tab.
- 124 1 and Figs. 3–5). Members of these genera (Gymnotoceras, Frechites and Parafrechites in
- particular) are sometimes hard to differentiate. They mainly differ in the ventral conch outline,
- ornamentation, adult ribbing and maximum growth size. The younger the individuals are, the
- 127 greater the similarities. Despite their complicated taxonomy, all selected species are index fossils
- of the late Anisian Fossil Hill Member (see Fig. 2). It was assumed that the individual species
- have similar coiling rates (i.e., the individual species develop the same number of whorls in the
- 130 course of their life). The total number of volutions developed by the species varies between five
- and a half and seven (see Tab. 1-Total number of volutions).
- 132 **Preparation and data acquisition.** We prepared high-precision cross-sections intersecting the
- protoconch of each specimen, following the methods by Klug et al. (2015) and Korn (2010).
- Subsequently, we scanned the polished surfaces in high resolution with a flat screen scanner to
- ensure that all pictures have the same scale. Thereafter the scan images were digitized. CT scan
- images of Anisian ammonoids from Nevada do not provide sufficient contrast of the internal
- 137 structures for a reliable analysis (Bischof & Lehmann 2020).
- Based on the digitized cross-sections we performed a 2D landmark-based geometric
- morphometrics analysis. The landmarks were retrieved in tpsDig2 v.2.31 (Rohlf 2010). Sixteen
- landmarks were digitized per half whorl (i.e. growth stage), which results in 176 landmarks per
- specimen (16 landmarks on 11 half whorls; Fig. 6). This set of landmarks consists of two single
- 142 (1, 2) and 7 pairs of landmarks (3–16), of which eight are sliding semi-landmarks. In order to
- omit missing values in subsequent analyses, the data set was limited to growth stage number 5.5.
- 144 From a methodological point of view, it is more practical to rotate the shells by 90° compared to
- 145 conventional orientation (cf. Stridsberg 1990). Since ammonoid conchs are spiral-shaped, each
- 146 whorl is cut in two parts when preparing the cross sections. Therefore, the conch is divided into a
- 147 left (whorls with odd numbers, here 0.5–5.5; "odd whorls") and a right (whorls with even
- numbers, here 1.0–5.0; "even whorls") part. Homologous landmarks were set in accordance to
- 149 the axial plane.
- 150 Calculation of Procrustes shape. All geometric morphometric analyses were done using the R
- software v 3.6.3. (R Core Team 2020) packages Morpho v2.8 (Schlager 2017), geomorph v3.3.1.
- 152 (Adams et al. 2020) and *RRPP* v0.6.0 (Collver & Adams 2018; Collver & Adams 2020). Plots
- were drawn with the R package ggplot2 (Wickham 2016). Using the *Morpho::procSvm* function,
- the 2D landmark coordinates were subjected to a full generalized Procrustes alignment (GPA).
- 155 The full Procrustes fit standardizes size, orientation and position, leaving only the Procrustes
- shape coordinates (Hammer & Harper 2005). Since the "odd" and "even" whorls cannot be made



- 157 congruent by any of these operations (i.e. alignment, translation, rotation), all "even" whorls
- were manually mirrored before the GPA.
- 159 The individual whorls were regarded as different structures of the ammonoid conch. Therefore,
- the GPA was performed separately for every whorl. The *procSym* function performs Procrustes
- superimposition including sliding of semi-landmarks on curves and accounts for the symmetry of
- the object. Subsequently, the R function geomorph::combine.subsets was used to normalize the
- 163 configurations of all growth stages to unit centroid size or with a customized weighting (see
- "Developmental morphospaces"). The centroid size (CS) is regarded as a proxy for the size of
- the whorls and equals the square root of the summed squared distances of each landmark from
- the centroid of the landmark configuration before the GPA (Zelditch et al. 2012).
- 167 To visualize the multivariate data in a two-dimensional morphospaces we ran a principal
- 168 component analysis (PCA) on the aligned Procrustes shape coordinates using the R function
- stats::prcomp. Thereby we used two different types of morphospaces: Ontogenetic and
- 170 developmental morphospaces.
- 171 Ontogenetic morphospaces. It is well-known that ammonoids have a very characteristic but
- also complex ontogenetic development (e.g., Klug 2001). To visualize the ontogenetic
- development of ammonoids there are different types of morphospaces. Ontogenetic
- morphospaces, as defined by Bischof & Lehmann (2020, p.2), illustrate the differences in total
- ontogenetic development of individuals. They show the data in an artificial state of combined
- morphologies of different ontogenetic stages. To calculate an ontogenetic morphospace, all
- 177 Procrustes shapes (i.e. whorls) of an individual are re-assembled before running the principal
- 178 component analysis. This means that, in an ontogenetic morphospace, the ontogenetic trajectory
- of every individual is reduced to a single data point. Ontogenetic morphospaces are a tool to
- examine if the ontogenetic pathways of individuals differ, but they do not show how the
- 181 trajectories vary.
- **Developmental morphospaces.** Developmental morphospaces as defined by Eble (2003, p. 40)
- are morphospaces that directly contain developmental information. In terms of this study this
- means that every individual dot in the morphospace reflects a specific ontogenetic stage (i.e.
- whorl) of an individual. By connecting all points of an individual, the ontogenetic trajectory can
- be obtained. In contrast to ontogenetic morphospaces, developmental morphospaces show how
- individual whorls differ from each other.
- As can be seen in Figure 6, size differences between different growth stages are tremendous. The
- 189 General Procrustes Analysis (GPA) removes all information about size from a given set of data
- 190 leaving only the pure shape coordinates. If normalized to unit centroid size (i.e. non-weighted
- morphospace), the earliest whorls of ammonoids get enormously enlarged and the last whorls
- scaled down. In general, deviations (measurement uncertainties as well as actual morphological
- variation) are increased for the initial whorls and reduced for older growth stages. Therefore, a
- second morphospace with weighted Procrustes shape coordinates was calculated. Thereby, the
- logarithmic centroid size ($log_{10}CS$) of all configurations of a growth stage were normalized to the
- proportional centroid size of the respective stage to the sum of all growth stages (log₁₀CS_{whorl i}/

- 197 $\sum \log_{10} CS_{\text{whorls}}$). The principal components of the PCA on the weighted shapes were called wPC
- 198 (weighted principal components).
- 199 If the relative $log_{10}CS$ is used to normalize the centroid size of the configurations, this approach
- 200 is extremely similar to a relative warp principal component analysis (RW-PCA) after
- 201 Mitteroecker et al. (2004). To calculate a RW-PCA the shape matrix of a configuration is
- augmented by an additional column containing information about the $log_{10}CS$ of the
- 203 configurations. Whereas the R function *geomorph::combine.subsets* scales every configuration
- accordingly, the size information in the RW-shape matrices are stored in the additional variable.
- 205 The resulting RW size-shape space can be analyzed with an ordinary PCA. Typically, RW size-
- shapes are strongly dominated by the log₁₀CS and PC1 therefore often accounts for more than 90
- 207 % of the variation. If proportional $log_{10}CS$ -values ($log_{10}CS_{configuration i} / \sum log_{10}CS_{configurations}$), are
- 208 used the analysis is less dominated by size, but the eigenvalues are very similar to the ones of the
- weighted PCA (wPCA). For simplicity the R function was used here.
- 210 Because weighting does not change the shapes itself, weighted and non-weighted developmental
- 211 morphospaces look very similar. The main difference is the placement of the individual
- 212 configurations within the morphospace. Whether weighted or non-weighted shape coordinates
- 213 should be used, depends on what the analysis is intended to show. Whereas wPCA adds an
- 214 allometric component to the analysis and maximizes the morphologic disparity between the
- 215 growth stages, it minimizes the variation within the individual stages. Furthermore, it may
- 216 suppress potential variation in the earliest stages.
- 217 To model the shapes at the maximum and minimum PC-values, the R function
- 218 GeometricMorphometricsMix::reversePCA (Fruciano 2019) was used. The function is designed
- 219 to recalculate artificial Procrustes shape variables from the extreme PC-values in a morphospace.
- 220 The thin-plate spline deformation grids were calculated using the R function
- 221 *geomorph::plotRefToTarget*.
- 222 Trajectory analysis. In morphometric studies, ontogenetic trajectories represent a series of
- 223 measurement values of different ontogenetic stages of an individual or a group, called
- 224 longitudinal data (Klingenberg 1998). To quantify the differences of the ontogenetic trajectories
- of the individual species, the R function RRPP::trajectory.analysis with 999 iterations was used.
- 226 The function calculates a linear model with at least one categorical interaction variable (here:
- 227 Shape ~ Species * GrowthStage) and assesses differences in path distance (magnitude
- 228 differences), shape of the trajectories and the angle between the individual trajectories (trajectory
- 229 correlation) (Collyer & Adams 2013).
- 230 If weighted shape-coordinates were used, the artificial size-shape relationship could overlay true
- 231 differences between the trajectories. Therefore, only non-weighted shape coordinates were
- 232 analyzed in the trajectory analysis.

Results

- 235 Ontogenetic morphospaces. Ontogenetic morphospaces are a mean to visualize whether the
- ontogenetic development of two or more individuals differ. Thereby, the ontogenetic trajectory



- of each specimen is reduced to one single point in the diagram. The first three components (PCs)
- of the Principal Component Analysis (PCA) on the shape coordinates with combined ontogenetic
- stages of an individual account for 58.3 % ($PC_1 = 38.3$ %, $PC_2 = 13.4$ %, $PC_3 = 6.6$ %) of the
- 240 total variation.
- 241 The convex hulls of the ontogenetic morphospace of most species reveal a large overlap (Fig. 7).
- 242 Considering that there is a total of 352 primary components (x and y coordinates of 176
- landmarks), but only 72 specimens, this result can be regarded as satisfactory.
- 244 Since PC1 accounts for 38.3 % of the total variation, the most important characteristic is the
- position of the individuals on the x-axis. In fact, there are certain species that primarily have
- 246 negative PC1 values (B. vogdesi, F. nevadanus, F. occidentalis, M. spinifer, P. meeki) and some
- 247 that are more restricted to positive PC1 values (G. blakei, G. mimetus, G. rotelliformis, G.
- 248 weitschati, P. dunni). B. cordeyi and D. lawsoni, both cover a wider range of different PC1
- values, but are generally restricted to negative PC2 and positive PC3 values.
- 250 Non-weighted developmental morphospace occupation. The first three components of the
- 251 Principal Component Analysis (PCA) on the non-weighted shape space account for 93.8 % (PC₁)
- 252 = 78.5 %, $PC_2 = 11.5 \%$, $PC_3 = 3.1 \%$) of the total variation. The PCA plot (Fig. 8) of PC1 and
- 253 PC2 shows that the whorls of early ontogenetic stages cover the lower left quadrant of the
- 254 morphospace (negative PC1 and PC2 values), which characterizes extremely depressed, broad
- 255 whorls with a flat venter (Fig. 9A). The center of the morphospace (PC1 equals 0 and PC2 is
- positive) is occupied by intermediate growth stages (juveniles), which have more quadratic
- outline with an only slightly triangular venter (Fig. 9B). The lower right quadrant (high PC1 and
- low PC2 values) is associated with the latest ontogenetic stages (adults). Towards maturity, the
- 259 whorls increase mainly in height and have a clearly triangular and sometimes a keel (Figs. 9C,
- 260 10). Overall, there are two extreme adult shapes: Type (A) describes rather depressed, stout
- 261 conches with only a slight overlap with the preceding whorl that are associated with much
- shorter ontogenetic trajectories and type (B) describes compressed conches with a clearly
- 263 triangular venter and a higher degree of overlap. Type B species are associated with longer
- ontogenetic trajectories. For the assignment of the species to the two types see Tab. 2.
- 265 The developmental morphospace of beyrichitine and paraceratitine ammonoids comprises three
- basic shape stages, which are not separated by sharp borders (Figs. 9): 1) Earliest whorls: broad
- and very flat; 2) Juveniles: more rounded and depressed; 3) Adults: mostly high and compressed
- 268 whorls. Since type A species stop their development at more rounded and depressed whorls, their
- adult whorls resemble the juvenile stages of type B (Fig. 10).
- 270 Ontogenetic trajectories in the non-weighted developmental morphospace. The ontogenetic
- trajectories of species in the non-weighted developmental morphospace share many similarities:
- 272 They all have the similar direction and a slight parabolic shape (Fig. 8). The variation detected
- by the trajectory analysis (R function *RRPP*::*trajectory.analysis*) revealed significant differences
- between the trajectories of most species (Additional file 1).
- 275 Members of the type A ontogeny have smaller magnitudes of shape change and different
- trajectory shapes than members from type B ontogeny (path distances A: 0.2005–0.0225a; B:



- 277 0.2276–0.2778). For the assignment of the species to the two types see Table 2. Only pairwise
- 278 differences of the path distance and the trajectory shape between type A and type B species are
- statistically significant (magnitude of shape change: 17 / 66 possible pairs; trajectory shape: 16 /
- 280 66 possible pairs).
- 281 Most species have statistically significant pairwise differences in trajectory slope (57 / 66
- possible pairs). Species of all pairs with non-significant pairwise p-values are in the same
- ontogenetic group (i.e. both belong to type A or B). The trajectories of the nine pairs with non-
- 284 significant differences in slope, have non-significant magnitudes and shapes also. However, none
- of the species that share a common slope have overlapping biostratigraphic ranges.
- 286 Weighted developmental morphospace occupation. The first three components of the
- 287 Principal Component Analysis (PCA) on the weighted shape space account for 94.8 % (wPC₁ =
- 288 85.8 %, wPC₂ = 7 %, wPC₃ = 3.0 %) of the total variation. In comparison to the regular PCA, the
- 289 wPCA is by definition more strongly controlled by the centroid size of the configurations,
- 290 which is mainly expressed by the domination of PC1.
- 291 Similar to the regular PCA plot (Fig. 8), the wPCA morphospace (Fig. 11) can be divided into
- three main parts: 1) The extremely depressed whorls of the earliest whorls cover the lower left
- 293 quadrant (low PC1 and PC2 values); 2) the center of the plot (PC1 equals 0, PC2 positive) is
- 294 occupied by the more depressed whorls of juveniles and 3) adult whorls are associated with
- 295 positive PC1 values. In contrast to the PCA, the wPCA reveals a more distinct separation of the
- 296 type A and type B groups of adult whorls (see Tab. 2). Representatives of the more depressed
- 297 type B clearly occupy the lower right quadrant (positive PC1 and negative PC2 values). This
- 298 division into type A and B can also be seen in the mean shapes of the whorl 5.5 of the respective
- 299 species (Fig. 10).

301

Discussion

- 302 Members of the family Ceratitidae show high intraspecific variation and strongly overlapping
- 303 morphospaces (Tab. 1, Figs. 3–5). The ornamentation, which is often regarded as essential for
- the description of Mesozoic ammonoid groups (Klug et al. 2015), is not a unique characteristic
- among the family Ceratitidae. A better feature to delineate members of this family appears to be
- 306 the shape of the whorl section. The latter, however, cannot be quantified adequately by
- traditional morphometric methods (Neige 1999). Accordingly, the utility of conventional
- 308 taxonomic and morphological methods is limited in this regard. Here we utilize landmarks and
- 309 semi-landmarks on ontogenetic cross-sections. The use of geometric morphometric methods
- 310 (GMM) with respect to their content of ontogenetic developmental information and their
- 311 usefulness in taxonomic descriptions were investigated.
- 312 Ontogenetic patterns in Ceratitidae. The ontogenetic trajectories of the studied species
- 313 comprise the tri-phasic development from strongly depressed to weakly depressed to compressed
- 314 whorl profiles (Figs. 8–11). Thereby, the studied species can be divided into two main
- ontogenetic groups: Type (A) Truncated trajectories that are associated with depressed adult
- 316 whorls; type (B) longer, complete trajectories that lead to a compressed adult whorl shape. The

PeerJ

- 317 process of lengthening and shortening of the trajectories (i.e. related to changes in rate and
- 318 timing of the development) account for the ontogenetic differentiation of the species in focus.
- 319 This contrasts a previous traditional morphometric analysis by Bischof & Lehmann (2020) of
- 320 ptychitids, which revealed that the spherocone-cadicone morphospace is much more distinct. The
- 321 highly ontogenetic differentiated genus *Ptychites* directly differed through characteristic
- 322 ontogenetic trajectories.
- While precise temporal growth rates of ammonoids are unknown (Knauss & Yacobucci 2014), a
- basic assumption herein was that the individual species have similar coiling rates (i.e., the
- 325 individual species develop the same number of whorls in the course of their life). Modified
- 326 rate/timing of shape change in relation to any ancestor, descendent respectively, within an
- evolutionary framework is called heterochrony (Zelditch et al. 2012, p.317). Interspecific
- variation of the species in focus arises from an acceleration, a special case of peramorphosis; (for
- 329 discussion of this term, see Alberch et al. 1979; McNamara 2012) that allows type B species to
- occupy an extended portion of the morphospace characterized by more compressed whorls.
- Therefore, the studied ceratitids do not primarily differ in shape, but rather in the timing of the
- development of individual shapes. Heterochrony as a mechanism in macroevolution is known to
- be a key driving factor in phenotypic diversification (i.e., Alberch et al. 1979; Gerber et al. 2007;
- 334 Gould 1977; Knauss & Yacobucci 2014; Korn et al. 2013; McKinney & McNamara 1991). The
- 335 quantification of the relationship between size and shape (i.e. heterochrony) will be the subject of
- 336 future studies.
- 337 Anisian ammonoid diversity. It is widely agreed that ammonoid diversity reached its maximum
- during the Triassic period (Brayard et al. 2009; House 1993; Whiteside & Ward 2011). Thereby,
- 339 the late Anisian ammonoid diversity peak was mainly dominated by members of the family
- 340 Ceratitidae (Brayard et al. 2009; supporting material fig. S2). However, there is a growing
- number of studies critically questioning diversity peaks by arguing that to some extent the
- 342 high diversity might be artificially inflated by taxonomic over-splitting (De Baets et al. 2013;
- 343 Forey et al. 2004; Knauss & Yacobucci 2014).
- 344 The results obtained here do justice to the general opinion that ontogenetic trajectories are a
- powerful tool to describe (e.g., Korn & Klug 2007) and discriminate ammonoid species (e.g.,
- 346 Bischof & Lehmann 2020; Rieber 1962): The newly introduced methods succeeded in
- statistically discriminate the pre-defined ceratitid species. Therefore, the high diversity of the
- Anisian ammonoid assemblages of Nevada appears not to be artificially inflated and the alpha
- taxonomy is regarded to be reasonable. However, the high morphological resemblances of the
- 350 investigated species cannot be denied. Therefore, this study supports the main idea of McGowan
- 351 (2004); McGowan (2005) and Brosse et al. (2013) that taxonomic diversity and morphological
- 352 disparity need not necessarily be closely linked.
- 353 Why you should take the trouble. There is no doubt that preparation and analysis of
- ontogenetic cross sections involves a lot of work (Korn 2012). However, geometric
- 355 morphometric methods (GMMs) open the door to a new world of objectified, statistically
- 356 quantifiable descriptions. For example, in the case of the fauna described herein, conventional



357 descriptions and traditional morphometric methods did not succeed to differentiate species adequately. Landmarks and semi-landmarks, however, enable to statistically quantify shape 358 variations of entire morphologies (Neige 1999) and allow to analyze shape and size separately 359 (Hammer & Harper 2005). However, it is important to be aware of the fact that GMM carry no 360 361 direct biological information. They help to understand if and how configurations differ, but not what the underlying mechanisms for their morphological development are. Therefore, GMM 362 cannot be considered as being a phylogenetic or taxonomic tool per se. However, in the complex 363 discoidal morphospace landmark-based approaches have proven to be useful to evaluate a priori 364 defined taxonomic groups. 365 The high resolution of the ontogenetic trajectories of the herein studied material was achieved 366 owing to the accretionary planispiral growth of ammonoids with conservation of previous growth 367 stages (Korn 2012), which adds an intuitive and precise time-component to the analysis. Even 368 though it is likely that small-scale ontogenetic changes are overlooked at a measurement density 369 370 of one measurement per 180 degrees, it can be assumed that no major developmental steps were skipped (Tajika & Klug 2020). Leaving out complete ontogenetic stages would most likely 371 prevent the recognition of ontogenetic processes such as heterochrony. If, for example, only the 372 earliest and latest stages of the ceratitid development were analyzed, representatives of type A 373 and type B would differ fundamentally. The planispiral growth of many ammonoid conches 374 therefore not only adds a time component to the analysis, but more importantly ensures that no 375 important developmental steps were skipped. This reinforces the general opinion that ontogenetic 376 377 trajectories of ammonoids are a powerful tool to study evolutionary developmental concepts such 378 as ontogeny.

379 380

381

382 383

384

385

386

387 388

389

390 391

392

393

394

395

396

Conclusions

The Anisian ammonoid diversity peak was mainly dominated by the family Ceratitidae (Brayard et al. 2009; supporting material fig. S2). However, the individual ceratitid species show high intraspecific variation and sometimes completely overlapping morphospaces. Using conventional methods, individual ceratitid species are difficult to distinguish. It was therefore assumed that the high Anisian diversity in Nevada is artificially inflated by taxonomic over-splitting. Using a landmark-based geometric morphometric approach this study succeeded to differentiate the pre-defined taxonomic entities in the fossil material from the late Anisian Fossil Hill Member in Nevada, USA, Therefore, the high Anisian ammonoid diversity in western North America appears not to be unreasonably inflated. Furthermore, this study supports the hypothesis that taxonomic diversity and morphologic disparity of Triassic ammonoids were decoupled (Brosse et al. 2013; McGowan 2004; McGowan 2005). The largest interspecific differences of ceratitids are the result of alterations of the ontogenetic trajectories that are likely linked to heterochronic processes (i.e. differences in timing of ontogenetic changes). This means that the individual species of this group are not solely defined by the morphology they attain at a certain growth stage, but rather by the sum and timing of all of their ontogenetic stages. The statistical quantification of the relationship between size and shape (i.e. heterochrony) will be the subject of



- 397 future studies. These processes make an ad hoc distinction of the different species particularly
- 398 challenging.
- For a reliable traditional taxonomic identification of the species herein, it is necessary to have
- 400 several individuals (Silberling 1962) with different ages of the same species from the same
- stratum. It has proven to be essential to analyze morphological variation of ceratitids not only
- 402 between species but also across different ontogenetic stages. Therefore, the significance of
- 403 ontogenetic studies on ammonoids with regard to taxonomic implications cannot be dismissed.
- The geometric morphometric methods introduced herein represent a big leap towards more
- 405 quantitative and objective taxonomic descriptions of ammonoids.

Acknowledgements

- 408 We would like to thank D. Kuhlmann (now Messel, Germany) as former technician of the
- 409 Geowissenschaftliche Sammlung Bremen for mechanical preparation of the material collected by
- our working group. M. Krogmann (Bremen, Germany) is thanked for his broad support in the
- artwork for this article. We are indebted to K. Boos for statistical support and the introduction to
- 412 the R software. P. Embree (Orangevale, CA, USA) is thanked for broad support, including
- 413 organization of field-campaigns, scientific information and the permission to collect on his
- 414 private property. We thank the U.S. Department of the Interior, Bureau of Land Management
- 415 (BLM, Nevada State office, Winnemucca District) for permission to collect samples in the
- 416 Wilderness Study Area of the Augusta Mountains, Pershing County.

417 418

421

422

423

424

425

426

427

428 429

430

431

432

433

References

- Adams DC, Collyer ML, and A. K. 2020. Geomorph: Software for geometric morphometric analyses. R package version 3.2.1. https://cran.r-project.org/package=geomorph.
 - Alberch P, Gould SJ, Oster GF, and Wake DB. 1979. Size and shape in ontogeny and phylogeny. *Paleobiology* 5:296-317.
 - Bischof EA, and Lehmann J. 2020. Ontogenetic analysis of Anisian (Middle Triassic) ptychitid ammonoids from Nevada, USA. *Journal of Paleontology* 94:829-851.
 - Brayard A, and Bucher H. 2015. Permian-Triassic extinctions and rediversifications. In: Klug C, Korn D, De Baets K, Kruta I, and Mapes RH, eds. *Topics in Geobiology*. Dordrecht, Springer: 465-473.
 - Brayard A, Escarguel G, Bucher H, Monnet C, Brühwiler T, Goudemand N, Galfetti T, and Guex J. 2009. Good genes and good luck: Ammonoid diversity and the End-Permian mass extinction. *Science* 325:1118-1121.
 - Brosse M, Brayard A, Fara E, and Neige P. 2013. Ammonoid recovery after the Permian— Triassic mass extinction: a re-exploration of morphological and phylogenetic diversity patterns. *Journal of the Geological Society* 170:225-236.
- Bucher H. 1992. Ammonoids of the *Shoshonensis* Zone (Middle Anisian, Middle Triassic) from northwestern Nevada (USA). *Jahrbuch der Geologischen Bundesanstalt Wien* 135:425-436
- Collyer ML, and Adams DC. 2013. Phenotypic trajectory analysis: comparison of shape change patterns in evolution and ecology. *Hystrix* 24:75.



450

451

457 458

459

460

461

462

463

464

465

468

469

470

471

472

473

474

475

476

477

- Collyer ML, and Adams DC. 2018. RRPP: An R package for fitting linear models to highdimensional data using residual randomization. *Methods in Ecology and Evolution* 9:1772-1779.
- Collyer ML, and Adams DC. 2020. RRPP: Linear model evaluation with randomized residuals in a permutation procedure. *Available at* https://cran.r-project.org/web/packages/RRPP.
- 444 Courville P, and Crônier C. 2005. Diversity or disparity in the Jurassic (Upper Callovian) genus 445 Kosmoceras (ammonitina): A morphometric approach. *Journal of Paleontology* 79:944-446 953.
- De Baets K, Klug C, and Monnet C. 2013. Intraspecific variability through ontogeny in early ammonoids. *Paleobiology* 39:75-94.
 - Eble GJ. 2003. Developmental morphospaces and evolution. In: Crutchfield JP, and Schuster PM, eds. *Santa Fe Institute Studies on the Sciences of Complexity*: Oxford University Press, 33-63.
- Forey PL, Fortey RA, Kenrick P, and Smith AB. 2004. Taxonomy and fossils: a critical appraisal.

 Philosophical Transactions of the Royal Society of London Series B: Biological Sciences
 359:639-653.
- Fruciano C. 2019. GeometricMorphometricsMix: Miscellaneous functions useful for geometric morphometrics. R package version 0.0.7.9000.
 - Gabb WM. 1864. Paleontology of California. *Description of the Triassic fossils of California and the adjacent territories*. Philadelphia: California Geological Survey, Paleontology:17-35.
 - Gerber S. 2017. The geometry of morphospaces: lessons from the classic Raup shell coiling model. *Biological Reviews* 92:1142-1155.
 - Gerber S, Neige P, and Eble GJ. 2007. Combining ontogenetic and evolutionary scales of morphological disparity: a study of early Jurassic ammonites. *Evolution & Development* 9:472-482.
 - Gould SJ. 1977. Ontogeny and phylogeny. Cambridge, Massachusetts: Harvard University Press:1-501.
- Hammer Ø, and Harper D. 2005. Paleontological data analysis. 2 ed. Cambridge, Blackwell:1-368.
 - House MR. 1993. Fluctuations in ammonoid evolution and possible environmental controls. In: House MR, ed. *Systematics Association Special Volume*. Oxford, Clarendon Press:13-34.
 - Jenks JF, Monnet C, Balini M, Brayard A, and Meier M. 2015. Biostratigraphy of Triassic ammonoids. In: Klug C, Korn D, De Baets K, Kruta I, and Mapes RH, eds. *Topics in Geobiology*. Dordrecht: Springer:329-388.
 - Johnston MR, Tabachnick RE, and Bookstein FL. 1991. Landmark-based morphometrics of spiral accretionary growth. *Paleobiology*:19-36.
 - Klein C, and Korn D. 2014. A morphometric approach to conch ontogeny of Cymaclymenia and related genera (Ammonoidea, Late Devonian). *Mitteilungen aus dem Museum für Naturkunde in Berlin Fossil Record* 17:1-32.
- Klingenberg CP. 1998. Heterochrony and allometry: the analysis of evolutionary change in ontogeny. *Biological Reviews* 73:79-123.
- 481 Klug C. 2001. Life-cycles of some Devonian ammonoids. *Lethaia* 34:215-233.
- Klug C, Korn D, Landman N, Tanabe K, De Baets K, and Naglik C. 2015. Describing ammonoid conchs. In: Klug C, Korn D, De Baets K, Kruta I, and Mapes RH, eds. *Topics in Geobiology*. Dordrecht: Springer.
- Knauss MJ, and Yacobucci MM. 2014. Geographic Information Systems technology as a morphometric tool for quantifying morphological variation in an ammonoid clade.

 Palaeontologia Electronica 17:1-27.
- 488 Korn D. 2010. A key for the description of Palaeozoic ammonoids. Fossil Record 13:5-12.



498

499

500

501

502

503

504

505

506

507 508

509

510

511

512

513

514

515

516

517

518

519

520

521

522

523

524

525

526

527

528

529

530

- Korn D. 2012. Quantification of ontogenetic allometry in ammonoids. *Evolution & Development* 490 14:501-514.
- Korn D, Bockwinkel J, Ebbighausen V, and Walton SA. 2013. Rare representatives in the ammonoid fauna from Büdesheim (Cephalopoda, Eifel, Late Devonian) and the role of heterochrony. *Neues Jahrbuch für Geologie und Paläontologie-Abhandlungen* 269:111-124.
- Korn D, and Klug C. 2003. Morphological pathways in the evolution of Early and Middle Devonian ammonoids. *Paleobiology* 29:329-348.
 - Korn D, and Klug C. 2007. Conch form analysis, variability, morphological disparity, and mode of life of the Frasnian (Late Devonian) ammonoid *Manticoceras* from Coumiac (Montagne Noire, France). In: Landman N, Davis RA, and Mapes RH, eds. Dordrecht: Springer:57-85.
 - Korn D, and Klug C. 2012. Palaeozoic ammonoids—diversity and development of conch morphology. *Earth and life*: Springer:491-534.
 - McGowan AJ. 2004. Ammonoid taxonomic and morphologic recovery patterns after the Permian–Triassic. *Geology* 32:665-668.
 - McGowan AJ. 2005. Ammonoid recovery from the Late Permian mass extinction event. *Comptes Rendus Palevol* 4:517-530. https://doi.org/10.1016/j.crpv.2005.02.004
 - McKinney ML, and McNamara KG. 1991. Heterochrony. The Evolution of Ontogeny. New York: Springer Science+Businee Media:1-437.
 - McNamara KJ. 2012. Heterochrony: the evolution of development. *Evolution: Education and Outreach* 5:203-218.
 - Meek FB. 1877. Part I. Palæontology. In: King C, editor. Washington: Government Printing Office: 1-197.
 - Mitteroecker P, Gunz P, Bernhard M, Schaefer K, and Bookstein FL. 2004. Comparison of cranial ontogenetic trajectories among great apes and humans. *Journal of Human Evolution* 46:679-698.
 - Mojsisovics Ev. 1879. Vorläufige kurze Übersicht der Ammoniten-Gattungen der mediterranen und juvavischen Trias. *Verhandlungen der Kaiserlich-Königlichen Geologischen Reichsanstalt Wien*:133-143.
 - Mojsisovics Ev. 1888. Über einige japanische Trias-Fossilien. Vienna: Alfred Holder, K.K. Hofund Universtitäts-Buchhändler:163-178.
 - Monnet C, Brayard A, and Brosse M. 2015. Evolutionary trends of Triassic ammonoids. In: Klug C, Korn D, De Baets K, Kruta I, and Mapes RH, eds. *Topics in Geobiology*. Dordrecht: Springer:25-50.
 - Monnet C, and Bucher H. 2005. New Middle and Late Anisian (Middle Triassic) ammonoid faunas from Northwestern Nevada (USA): Taxonomy and biochronology. *Fossils and Strata* 52:1-121.
 - Monnet C, De Baets K, and Klug C. 2011. Parallel evolution controlled by adaptation and covariation in ammonoid cephalopods. *BMC Evolutionary Biology* 11 (115):1-21.
 - Naglik C, Monnet C, Goetz S, Kolb C, De Baets K, Tajika A, and Klug C. 2015. Growth trajectories of some major ammonoid sub-clades revealed by serial grinding tomography data. *Lethaia* 48:29-46.
- Neige P. 1999. The use of landmarks to describe ammonite shape. In: Olóriz F, and Rodríguez-Tovar FJ, eds. *Advancing Research an Living and Fossil Cepha/opods*. New York: Kluwer Academic/Plenum:263-272.
- Neige P. 2015. Events of Increased Biodiversity: Evolutionary Radiations in the Fossil Record. London & Oxford: ISTE Press Elsevier:1-152.
- Neige P, and Dommergues J-L. 1995. Morphometrics and phenetic versus cladistic analysis of the early Harpoceratinae (Pliensbachian ammonites). *Neues Jahrbuch für Geologie und* Paläontologie, Abhandlungen 196:411-438.

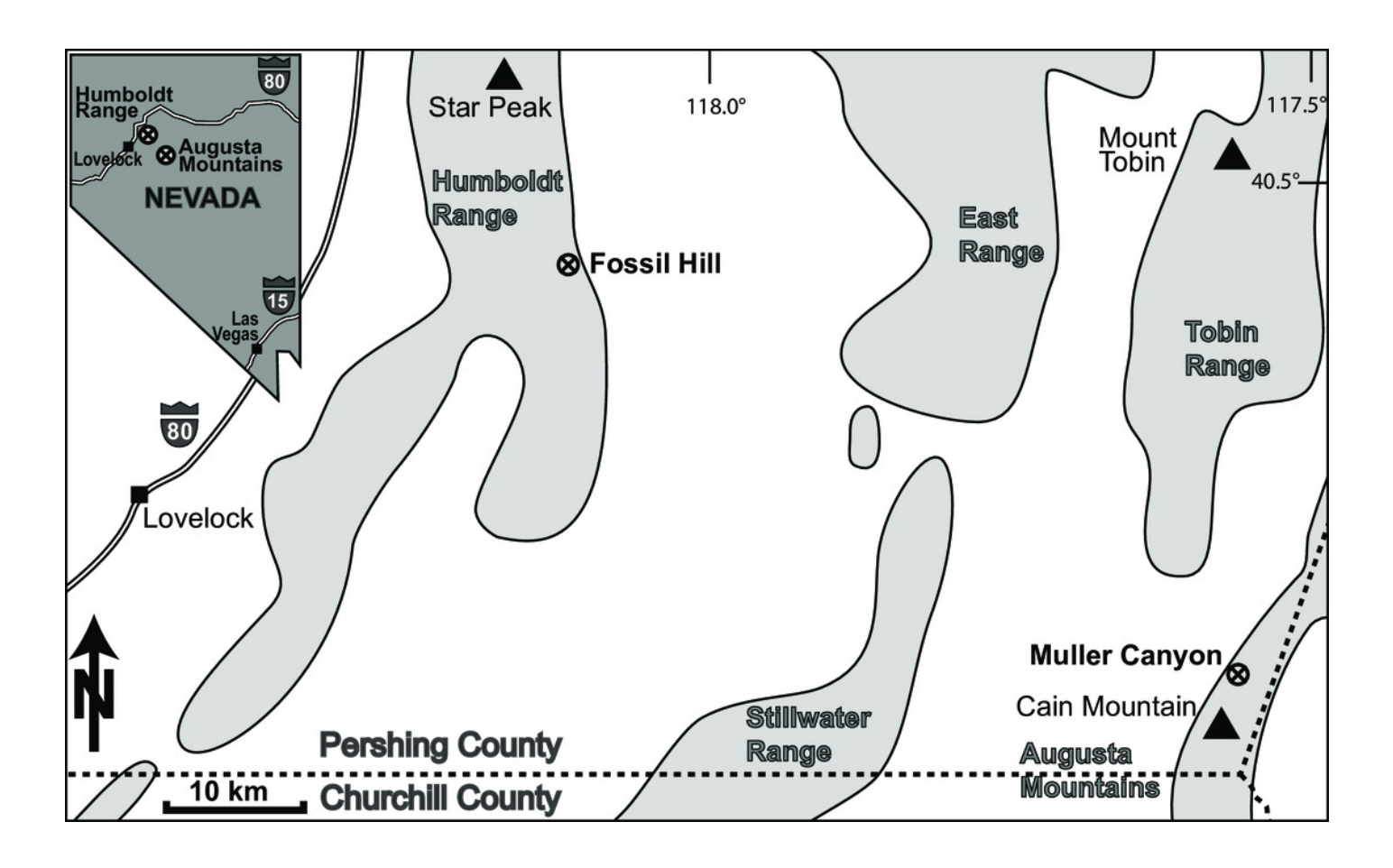


- Nichols KM, and Silberling NJ. 1977. Stratigraphy and depositional history of the Star Peak Group (Triassic), northwestern Nevada. *Special Paper Geological Society of America* 178:1-73.
- R Core Team. 2020. R: A Language and Environment for Statistical Computing. Version 3.6.3. Vienna, Austria: R Foundation for Statistical Computing.
- Raup DM. 1966. Geometric analysis of shell coiling: general problems. *Journal of Paleontology* 40:1178-1190.
 - Reyment RA. 2003. Morphometric analysis of variability in the shell of some Nigerian Turonian (Cretaceous) ammonites. *Cretaceous Research* 24:789-803.
 - Reyment RA, and Kennedy WJ. 1998. Taxonomic recognition of species of *Neogastroplites* (Ammonoidea, Cenomanian) by geometric morphometric methods. *Cretaceous Research* 19:25-42.
 - Rieber H. 1962. Beobachtungen an Ammoniten aus dem Ober-Aalénien (Systematik und Ontogenie). *Eclogae Geologicae Helvetiae* 55:587-594.
 - Rohlf F. 2010. TPSDig2: A program for landmark development and analysisAvailable at: http://life.bio.sunysb.edu/morph (accessed at January 30, 2018)).
 - Schlager S. 2017. Morpho and Rvcg Shape Analysis in R: R-Packages for Geometric Morphometrics, Shape Analysis and Surface Manipulations. In: Zheng G, Li S, and Székely G, eds.: Academic Press:217-256.
 - Silberling NJ. 1962. Stratigraphic distribution of Middle Triassic ammonites at Fossil Hill, Humboldt Range, Nevada. *Journal of Paleontology* 36:153-160.
 - Silberling NJ, and Nichols DJ. 1982. Middle Triassic molluscan fossils of biostratigraphic significance from the Humboldt Range, northwestern Nevada. *US Geological Survey Professional Paper*:1-77.
 - Simon MS, Korn D, and Koenemann S. 2010. Disparity fluctuations in Jurassic ammonoids by means of conch geometry. *Palaeogeography, Palaeoclimatology, Palaeoecology* 292:520-531.
 - Simon MS, Korn D, and Koenemann S. 2011. Temporal patterns in disparity and diversity of the Jurassic ammonoids of southern Germany. *Fossil Record* 14:77-94.
 - Smith JP. 1914. The Middle Triassic marine invertebrate faunas of North America. Washington:1-254.
 - Spath LF. 1934. Catalogue of the fossil Cephalopoda in the British Museum (Natural History): Part IV The Ammonoidea of the Trias. London: British Museum of Natural History:1-521.
 - Stone JR. 1998. Landmark based thin plate spline relative warp analysis of gastropod shells. *Systematic Biology* 47:254-263.
 - Stridsberg S. 1990. Orientation of cephalopod shells in illustrations. *Palaeontology* 33:243-248.
 - Tajika A, and Klug C. 2020. How many ontogenetic points are needed to accurately describe the ontogeny of a cephalopod conch? A case study of the modern nautilid *Nautilus pompilius*. *PeerJ* 8:e8849.
 - Tajika A, Morimoto N, Wani R, Naglik C, and Klug C. 2015. Intraspecific variation of phragmocone chamber volumes throughout ontogeny in the modern nautilid Nautilus and the Jurassic ammonite Normannites. *PeerJ* 3:e1306.
 - Van Bocxlaer B, and Schultheiß R. 2010. Comparison of morphometric techniques for shapes with few homologous landmarks based on machine-learning approaches to biological discrimination. *Paleobiology* 36:497-515.
 - Whiteside JH, and Ward PD. 2011. Ammonoid diversity and disparity track episodes of chaotic carbon cycling during the early Mesozoic. *Geology* 39:99-102.
- Wickham H. 2016. ggplot2: elegant graphics for data analysis: springer.
- Zelditch ML, Swiderski DL, and Sheets HD. 2012. Geometric morphometrics for biologists: a primer. 2 ed. London, Waltham & San Diego: Academic Press:1-478.



Manuscript to be reviewed

Location of the study area in NW Nevada, USA. The Fossil Hill and the Muller Canyon localities are marked. Figure adapted from (Bischof & Lehmann 2020); fig. 1).

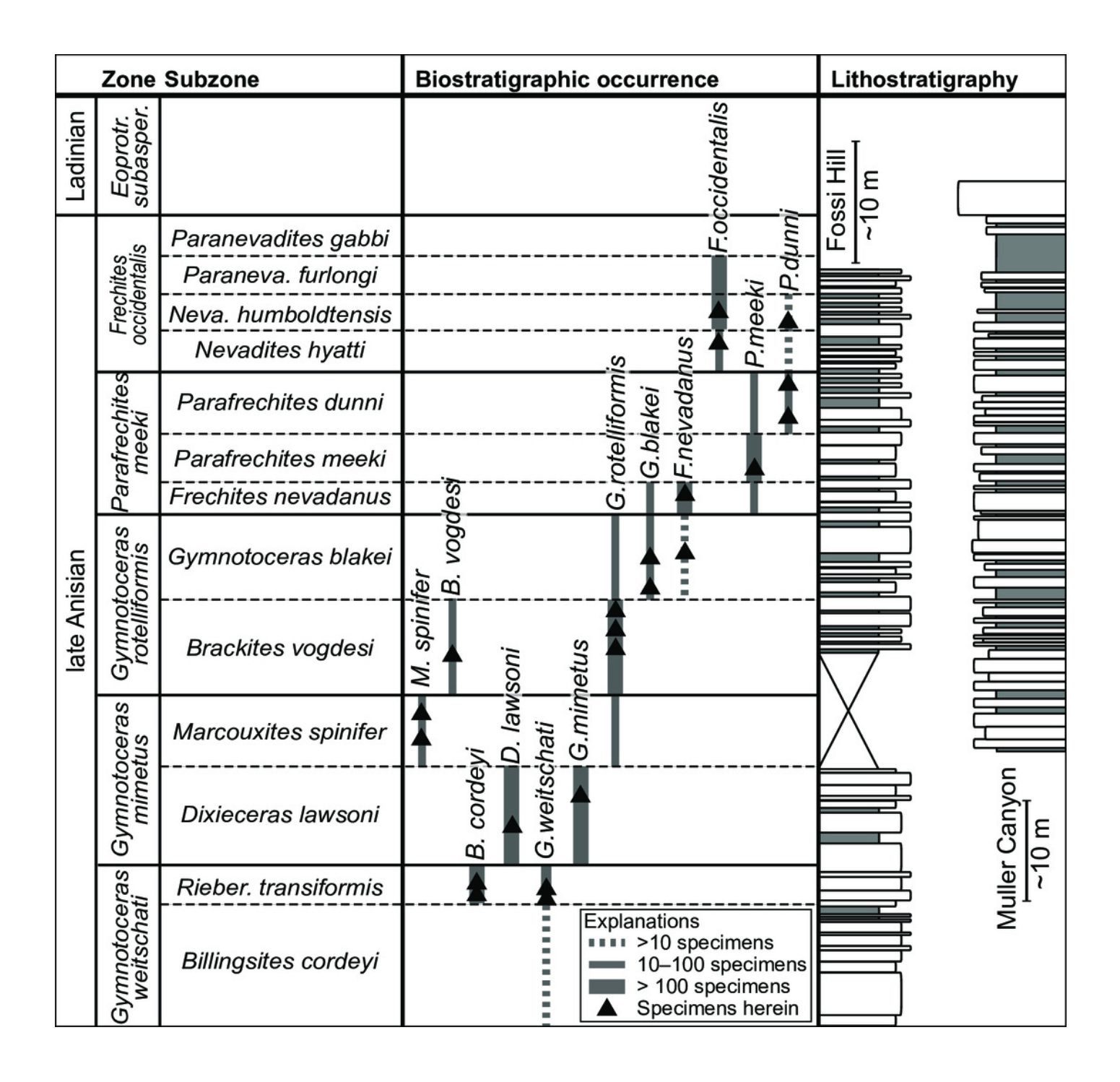




Biostratigraphic distribution of fossil material and synoptic lithostratigraphic sections of the outcrops in the Muller Canyon and Fossil Hill area. Stratigraphic section of Muller Canyon adapted from (Bischof & Lehmann 2020); fig. 2).

Gray areas in stratigraphic column: Calcareous siltstone; white areas: lenticular limestone, box width refers to weathering profile.

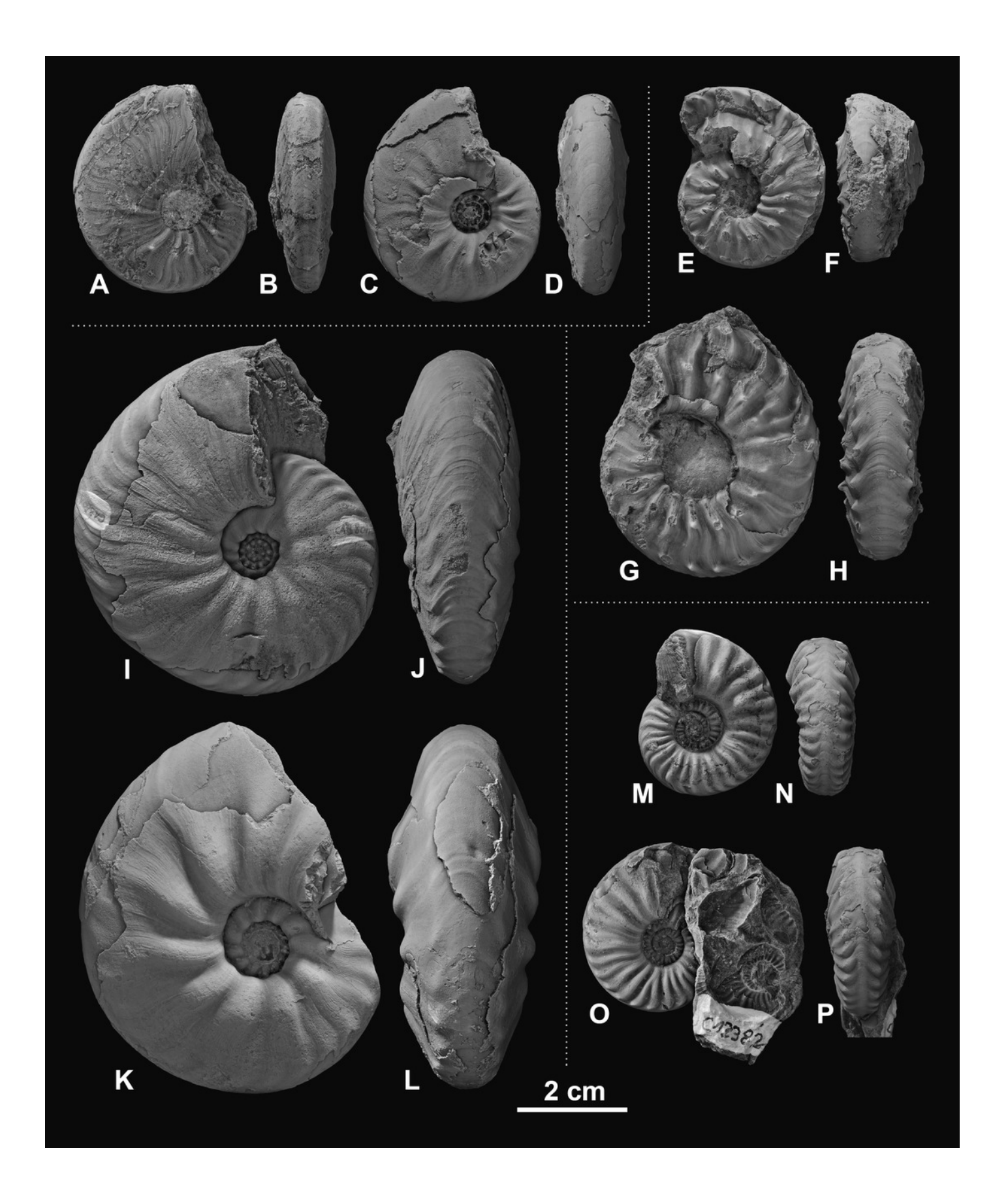






Ceratitid ammonoids from the Anisian (Middle Triassic) Fossil Hill Member of NW Nevada, USA.

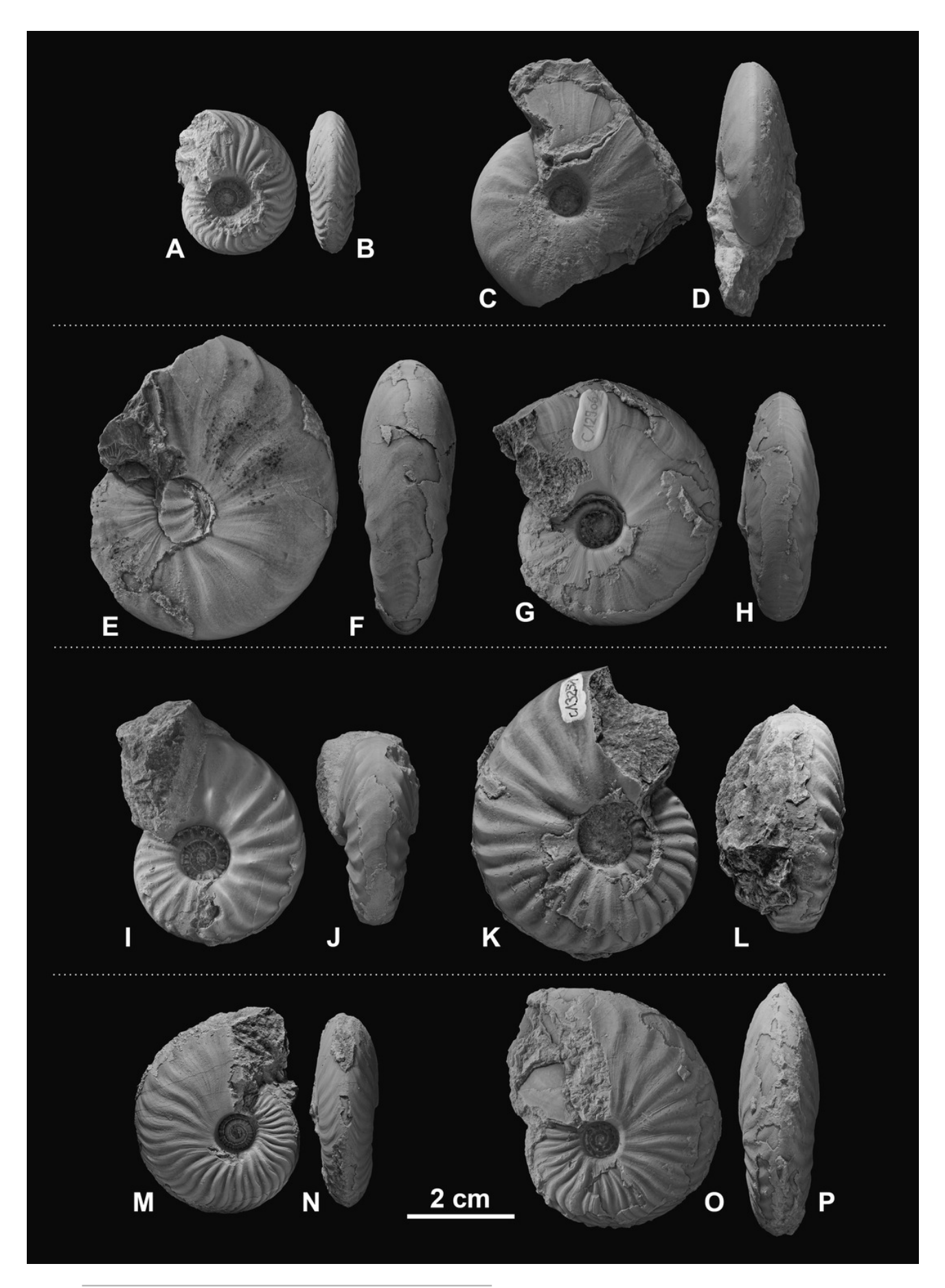
A-D: Billingsites cordeyi Monnet & Bucher, 2005, (A, B) GSUB C11082, (C, D) GSUB C11517; E-H: Brackites vogdesi (Smith, 1904), (E, F) GSUB C11649, (G, H) GSUB C11646; I-L: Dixieceras lawsoni (Smith, 1914), (I, J) GSUB C13801, (K, L) GSUB C13805; M-P: Frechites nevadanus (Mojsisovics 1888), (M, N) GSUB C12377, (O, P) GSUB C12382.





Ceratitid ammonoids from the Anisian (Middle Triassic) Fossil Hill Member of NW Nevada, USA.

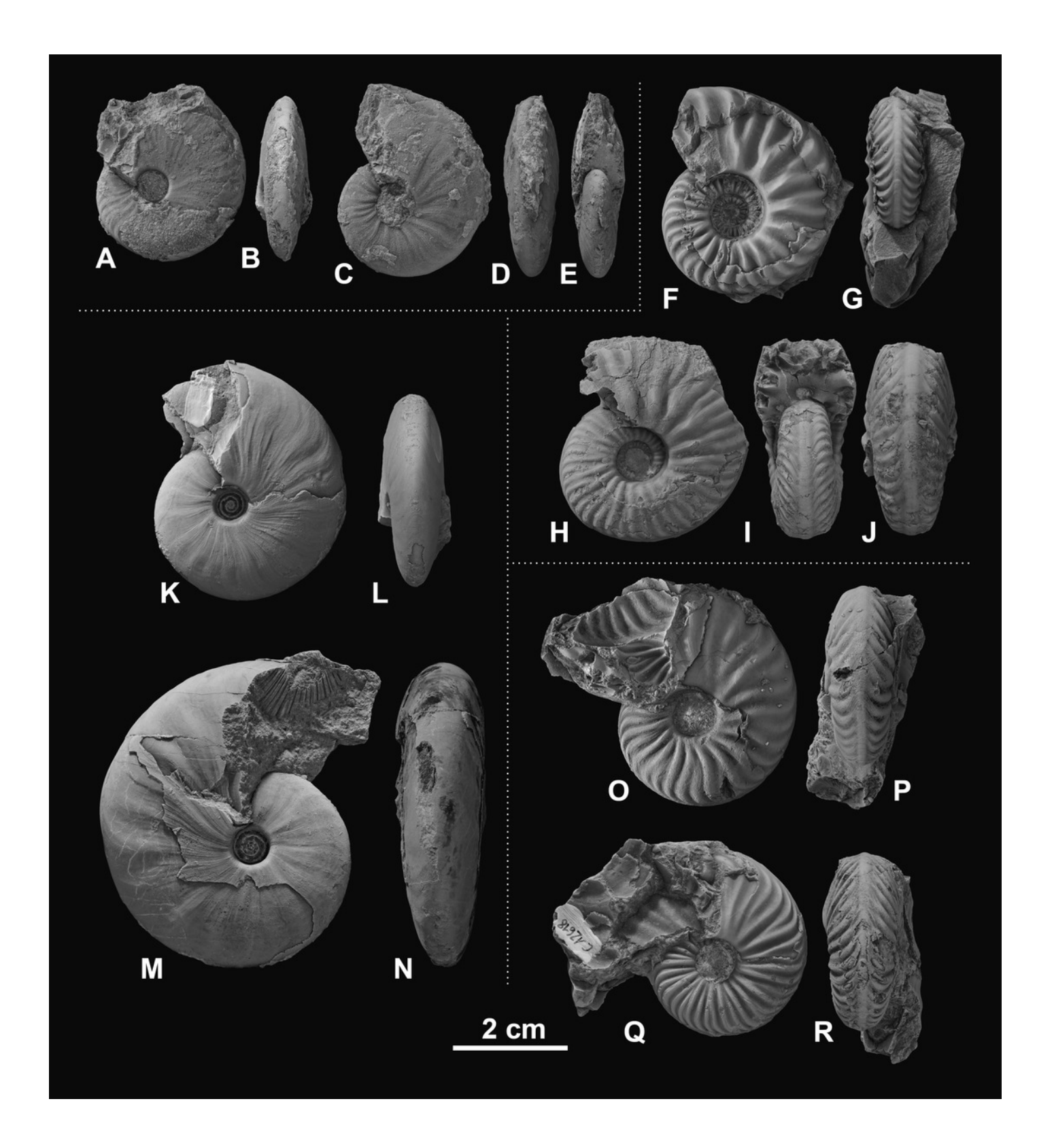
A-D) Gymnotoceras blakei (Gabb, 1864), (A, B) GSUB C12243, (C, D) GSUB C12264; E-H: Parafrechites dunni (Smith, 1914), (E, F) GSUB C9946 (G, H) GSUB C12906; I-L: Frechites occidentalis (Smith 1914), (I, J) GSUB C8998, (K, L) GSUB C13251; M-P: Gymnotoceras rotelliformis (Meek, 1877), (M, N) GSUB C11594, (O, P) GSUB C11702.





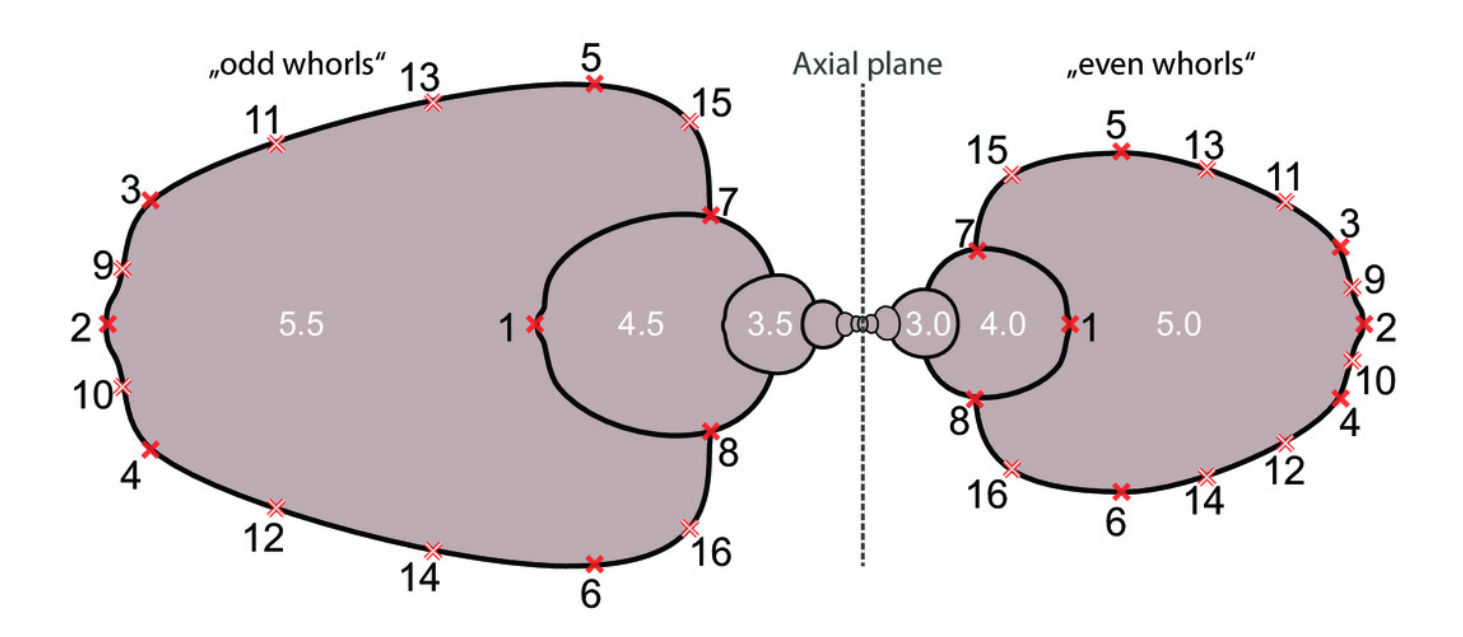
Ceratitid ammonoids from the Anisian (Middle Triassic) Fossil Hill Member of NW Nevada, USA.

A-E: *Gymnotoceras weitschati* Monnet & Bucher 2005, (A, B) GSUB C11111, (C-E) GSUB C11158; F-J: *Marcouxites spinifer* (Smith, 1914), (F, G) GSUB C10050, (H-J) GSUB C10137; K-N: *Gymnotoceras mimetus* Monnet & Bucher 2005, (K, L) GSUB C15005, (M, N) GSUB C13811; O-R: *Parafrechites meeki* (Mojsisovics 1888), (O, P) GSUB C12534, (Q, R) GSUB C12618.



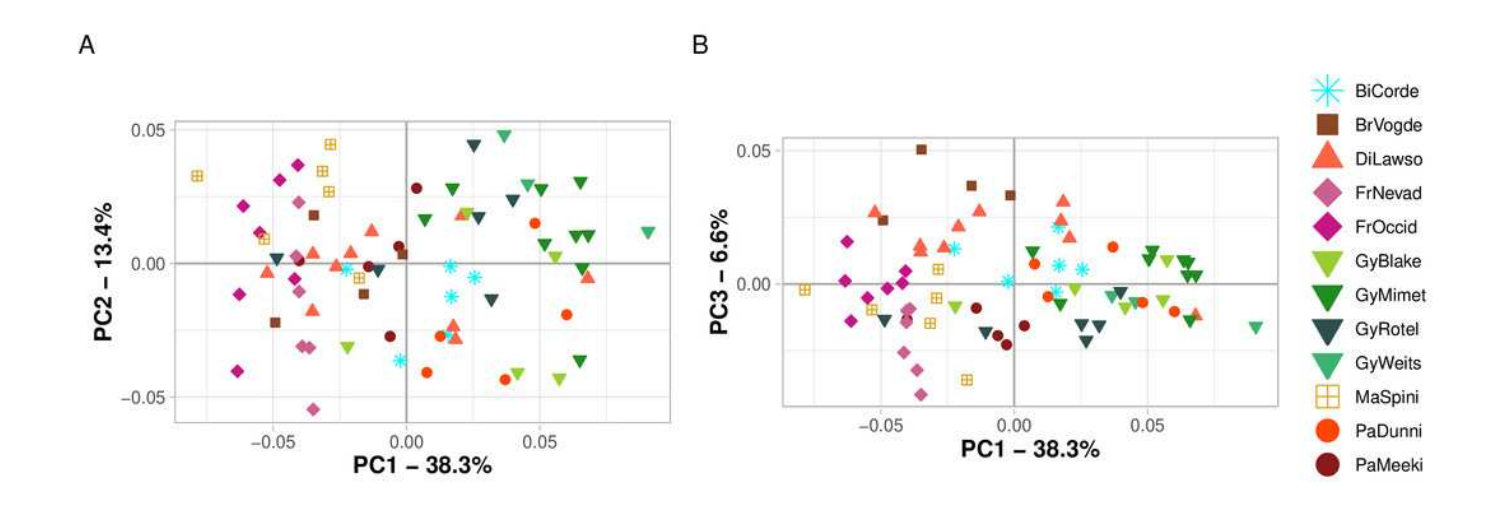
Digitized sketch of high-precision cross-section of an ammonoid specimen meeting the initial chamber (protoconch) with position of landmarks on last two half whorls. Filled crosses: fixed landmarks; empty crosses: sliding landmarks; black numbers: numbers

Definition of fixed landmarks: 1) venter of preceding whorl; 2) venter of whorl; 3 and 4) ventral shoulder or point of highest curvature; 5 and 6) maximum width; 7 and 8) Umbilical seam

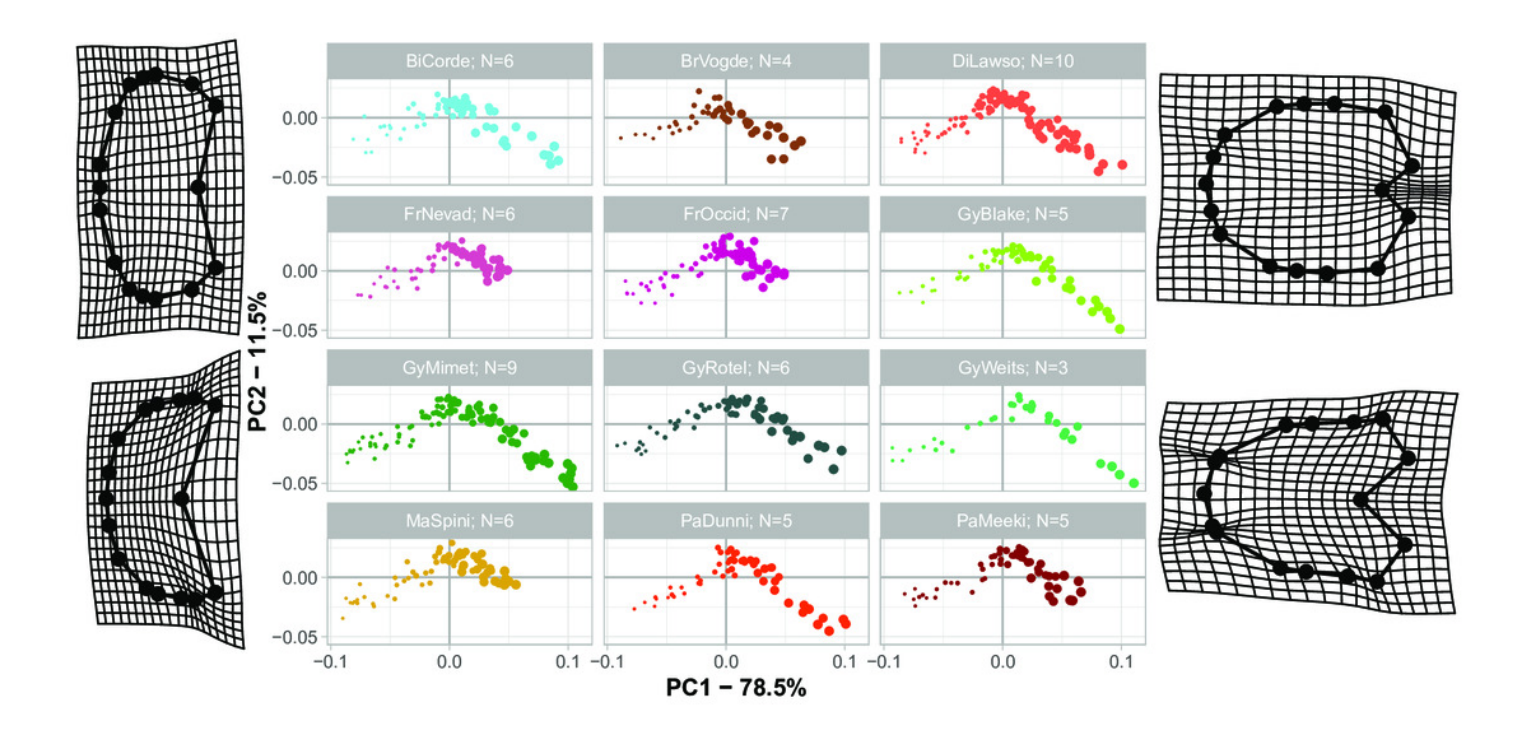




Ontogenetic morphospace of all species analyzed. A) Principal Component 1 and 2; B) Principal component 1 and 3.

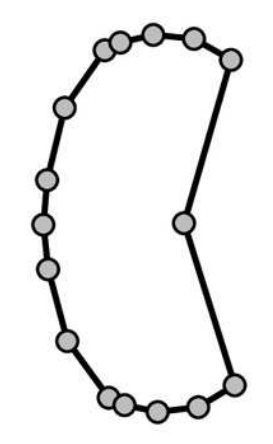


Developmental morphospace with PCA of Procrustes shape variables. Point size refers to growth stage. Deformation grids of the mean shape to the modeled shapes of the extreme values for PC1 and PC2.

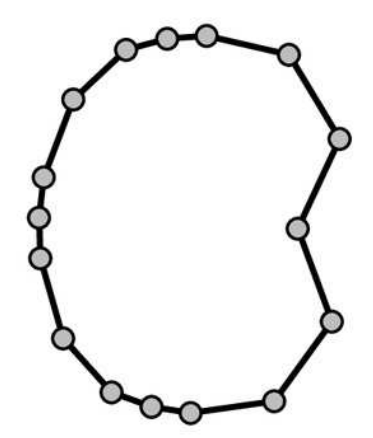


Mean shapes of growth stages 0.5, 3.0 and 5.5.

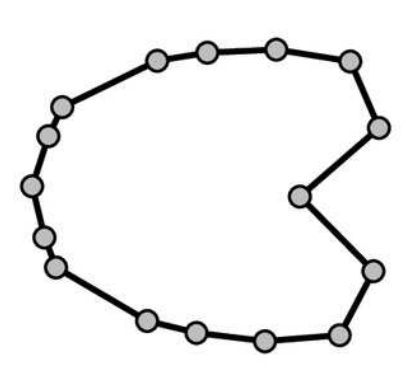
A) whorl 0.5



B) whorl 3.0

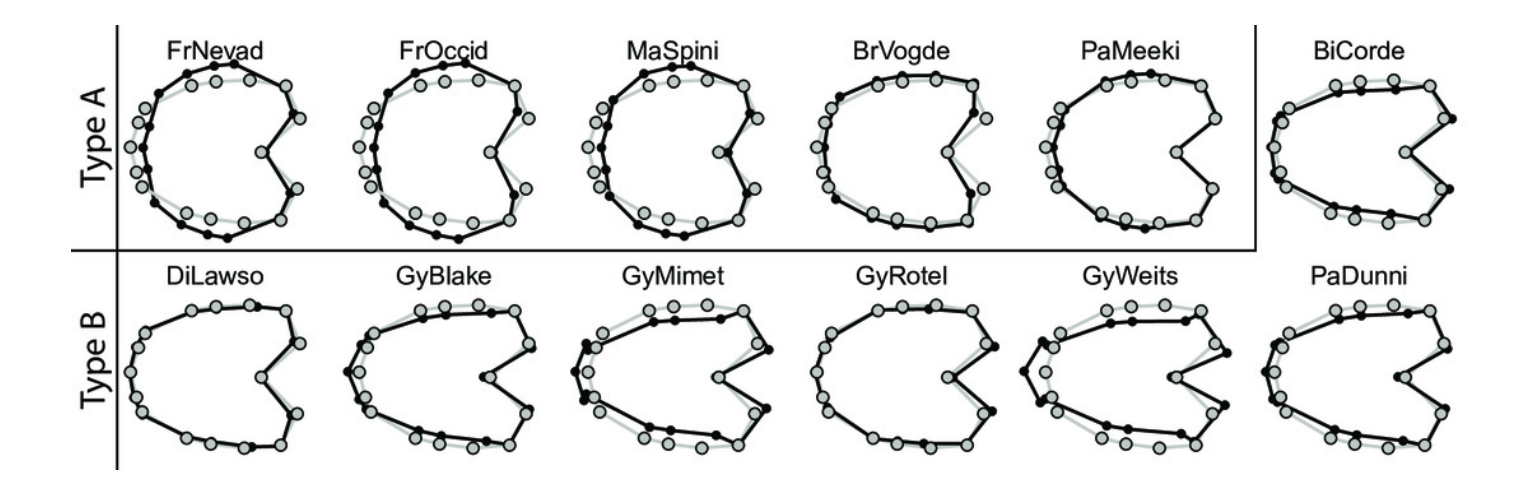


C) whorl 5.5





TPS spline of mean shape of whorl 5.5 of all species in this study (grey) plotted against the mean shape of whorl 5.5 of the respective species (black).



Developmental morphospace with PCA of weighted Procrustes shape variables. Point size refers to growth stage. Deformation grids of the mean shape to the modeled shapes of the extreme values for PC1 and PC2.

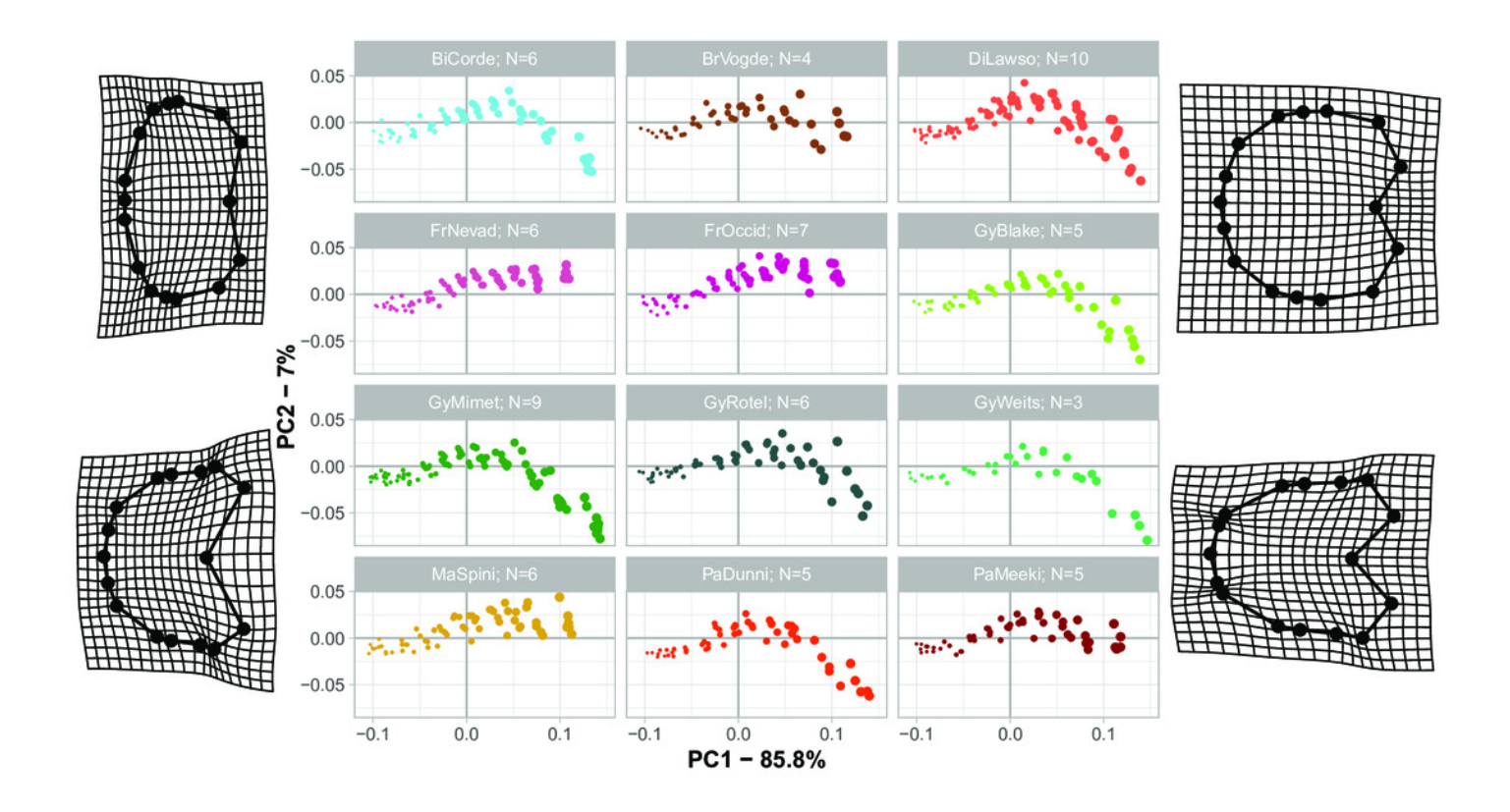




Table 1(on next page)

Morphological comparison of the species in focus. For biostratigraphic distribution see Figure 2.

N: Number of specimens; U: maximum umbilical diameter; W: maximum whorl width; D: maximum diameter of conch. Measurement values and ratios based on material herein. More detailed information on the studied species was published by Silberling & Nichols (1982) and Monnet & Bucher (2005).

Species	N	Total number of volutions	Venter and conch outline	Sculpture	Dmax [mm]	U/D	W/D	Figure herein
Beyrichitinae Spath, 1934								
Billingsites cordeyi Monnet & Bucher, 2005	6	6—6.5	Slightly angular ventral shoulder Very weak developed keel	Falcoid, prorsiradiate ribs, sometimes branched Nodes at branching points	34.3	min: 0.17 max: 0.24	min: 0.28 max: 0.35	3A-D
Dixieceras lawsoni (Smith, 1914)	10	6—7	Stout, discoidal outline Rounded ventral shoulders	Falcoid, prorsiradiate ribs, sometimes branched Umbilical thickening of whorls	57.7	min: 0.19 max: 0.25	min: 0.23 max: 0.44	3I–L
Frechites nevadanus (Mojsisovics 1888)	6	5.5—6	Subrectangular outline Clearly developed keel	Strong, falcoid, prorsiradiate ribs, sometimes branched Adults: Pronounced tubercles at lower flank	28.9	min: 0.29 max: 0.37	min: 0.39 max: 0.46	3M-P
Frechites occidentalis (Smith 1914)	7	6—7	Angular ventral shoulder Sometimes very weak developed keel	Strong, slightly prorsiradiate ribs, some rare tubercles Towards maturity ribbing fades	42.6	min: 0.24 max: 0.27	min: 0.38 max: 0.43	4I–L
Gymnotoceras blakei (Gabb, 1864)	5	5.5—6	Discoidal outline Rounded ventral shoulders, weak keel	Falcoid, prorsiradiate, unbranched ribs Towards maturity fading ribs and megastriae	37.8	min: 0.15 max: 0.28	min: 0.30 max: 0.38	4A–D
Gymnotoceras mimetus Monnet & Bucher 2005	9	6—6.5	Discoidal to subrectangular outline Rounded ventral shoulders, no keel	Megastriae and weak falcoid, prorsiradiate ribs, slightly swelling towards umbilicus	43.0	min: 0.14 max: 0.22	min: 0.29 max: 0.40	5K-N

Gymnotoceras rotelliformis (Meek, 1877)	6	6	Stout discoidal outline, very weak keel Rounded ventral shoulders	Regular, slightly prorsiradiate ribs Towards maturity ribbing slightly fades	34.3	min: 0.17 max: 0.26	min: 0.32 4 max: 0.38	4M–P
Gymnotoceras weitschati Monnet & Bucher 2005	3	6	Compressed, discoidal outline Perfectly rounded shoulders, no keel	Megastriae and weak falcoid, prorsiradiate ribs, slightly swelling towards umbilicus	28.4	min: 0.17 max: 0.20	min: 0.29 3 max: 0.33	5A–E
Parafrechites dunni (Smith, 1914)	5	5.5—6.5	Stout discoidal outline, sometimes keel Rounded to subangular ventral shoulders	Regular but weak, slightly prorsiradiate ribs Towards maturity ribbing slightly fades	35.2	min: 0.18 max: 0.20	min: 0.31 4 max: 0.42	4E–H
Parafrechites meeki (Mojsisovics 1888)	5	5.5—6	Subrectangular outline Strong keel, sub- angular shoulders	Strong and regular, falcoid, prorsiradiate ribs, sometimes branched	32.1	min: 0.22 max: 0.27	min: 0.34 3 max: 0.41	5O–R
Paraceratitinae Silberling, 1962								
Brackites vogdesi (Smith, 1904)	4	6—7	Subrectangular outline, slightly rounded shoulders	Regular, falcoid, branched, prorsiradiate ribs Tubercles at brancing point	29.6	min: 0.28 max: 0.37	min: 0.35 amax: 0.37	3E–H
Marcouxites spinifer (Smith, 1914)	6	5.5—6	Subrectangular outline, angular shoulder Clearly developed keel	Strong and regular, falcoid, prorsiradiate ribs Tubercles and spines at branching point	25.8	min: 0.26 max: 0.36	min: 0.38 s max: 0.42	5F–J



Table 2(on next page)

Summary and explanation on the three different ontogenetic types. Heterochronic terms as defined by McNamara (2012).



Type	Species	Heterochrony	Adult whorl shapes
A1	F. nevadanus F. occidentalis M. spinifer B. vogdesi P. meeki	Paedomorph	depressed, stout conches, only slight overlap with preceding whorl
В	B. cordeyi D. lawsoni G. blakei G. mimetus G. rotelliformis G. weitschati P. dunni	Peramorph (Acceleration)	compressed conches, more pronounced venter, more overlap with preceding whorl